

Programmable SDN-enabled S-BVT based on hybrid electro-optical MCM

L. Nadal, M. Svaluto Moreolo, J. M. Fàbrega, R. Casellas, F. J. Vílchez, R. Martínez, R. Vilalta and R. Muñoz

Abstract—A programmable SDN-enabled sliceable bitrate variable transceiver based on hybrid electro-optical multicarrier modulation as a key enabler for superchannel generation in future 5G metro networks is proposed. Multiple discrete multitone signals can be multiplexed/demultiplexed with optical orthogonal transform processors such as spectral selective switches (SSSs). By implementing optical spectrally-efficient transforms at the SSSs, we are able to generate a high capacity superchannel to support the transmission targets envisioned in 5G networks. Specifically, the optimal transform can be programmed by the control plane through the corresponding SDN agents by suitably configuring the phase and attenuation of the SSSs's ports. Furthermore, with the adoption of MCM formats, increased system/network flexibility is achieved. In this work, two different transceiver configurations have been proposed and assessed. They are based on intensity modulation with direct detection and amplitude modulation with coherent reception. A flexible receiver configuration selection is envisioned according to the target network requirements/condition.

Index Terms—Adaptive bit/power loading, Discrete multitone modulation, Optical superchannel, Wavelet transform

I. INTRODUCTION

In order to support the new emerging heterogeneous 5G services and the increasing mobile data traffic, which has grown 18-fold over the past 5 years, according to [1], current metro networks are evolving towards more convergent, scalable and flexible architectures [2], [3]. 5G era brings new optical transport network challenges including fast reconfigurability of transport resources, end-to-end latency shorter than 1 ms, very high data rate/capacity on-demand and fast reconfigurability of transport resources [4], [5]. Multicarrier modulation (MCM), such as orthogonal frequency division multiplexing (OFDM) and discrete multitone (DMT) schemes, arises as a promising technology to support high speed transmission envisioned in future 5G networks. Thanks to its sub-/super-wavelength

granularity, a high degree of reconfigurability and flexibility is achieved promoting an efficient network resource usage to reduce capital expenditures (CAPEX) and operational expenditures (OPEX). Moreover, by the adoption of the flex-grid paradigm, network/system flexibility can be further enhanced by using frequency slots of 12.5 GHz granularity, enabling dynamic bandwidth/channel allocation [6], [7].

Superchannel generation enables to exploit the flex-grid paradigm by multiplexing/allocating different signals/channels in a high-capacity single data flow according to the user requests in a spectrally-efficient and scalable manner. Multiple frequency slots of 12.5 GHz can be selected, providing customized spectral grids, according to the superchannel bandwidth occupation. The superchannel generation can be implemented either in optical or electrical domain [8]. In order to take benefit of both domains a hybrid approach can be envisioned [8]. Specifically, system flexibility is obtained at the sub-wavelength level by the implementation of bit and power loading (BL/PL) algorithms, which allows different modulation formats and power values per subcarrier according to the channel profile [9]. In order to also exploit super-wavelength granularity and meet the increased capacity and higher data rate demands of future 5G optical networks in a cost-effective manner, MCM superchannels can be generated in combination with direct-detection (DD). More complex optical implementations based on coherent (CO) detection can be also considered dealing with high data rate/reach targets [10]. On the other hand, programmable and adaptive sliceable bitrate variable transceivers (S-BVT), configured by following a software defined networking (SDN) paradigm, can be adopted as a key enabler of superchannel generation, also providing flexibility in the transport infrastructure by enabling a dynamic resource sharing [11], [12]. Specifically, the S-BVT consists of multiple rate/distance adaptive subtransceiver modules that can be enabled/disabled and programmed by an SDN controller through SDN agents for efficient resource usage to support variable traffic, allowing a dynamic management of optical networks [11], [12], [13]. Specifically, the aggregation of the multiple slices can be implemented in a spectrally-efficient manner by packing the MCM electrical signals into a superchannel using optical orthogonal transform processors based

This work has been partially funded by the European Commission through the H2020-ICT-2016-2 METRO-HAUL project (G.A. 761727) and the Spanish Ministry MINECO project DESTELLO (TEC2015-69256-R).

L. Nadal, M. Svaluto Moreolo, J. M. Fàbrega, R. Casellas, F. J. Vílchez, R. Martínez, R. Vilalta and R. Muñoz are with the Centre Tecnològic de Telecomunicacions de Catalunya (CTTC/CERCA), 08860 Castelldefels (Barcelona), Spain (e-mail: laia.nadal@cttc.es).

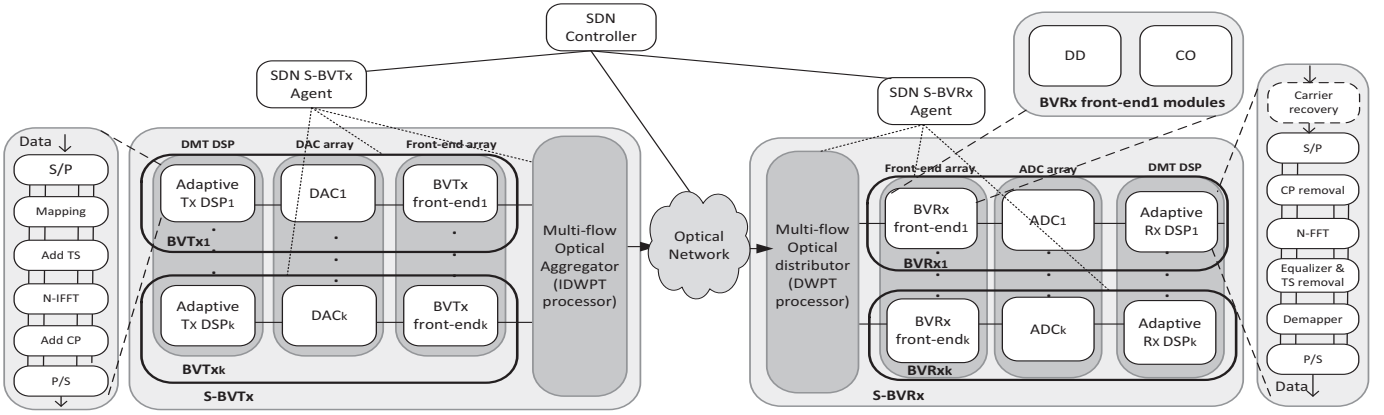


Fig. 1. Programmable SDN-enabled S-BVT architecture

on either the fast Fourier transform (FFT) or the discrete wavelet packet transform (DWPT) [14]. The DWPT is used to increase spectral efficiency (SE), as the multiple flows can be packed with no guard-band and unlike the FFT, the wavelet finite base functions present both time and frequency localization, enabling simpler implementation [15], [16]. As previously studied in the literature, in the case of implementing the DWPT, different wavelet bases can be selected to obtain different nonlinearity performance and chromatic dispersion (CD) tolerance [17]. Hence, the flexibility in the choice of the wavelets allows the use of optimal wavelets for each application.

The optical orthogonal transform processors can be implemented with spectral selective switches (SSSs), which can be part of either the transceiver or the network, and suitably programmed to implement the desired optical transform depending on the network condition and requirements [14]. Alternatively, cost/power efficient schemes such as planar lightwave circuit/photonic integrated circuit (PIC) devices can also be considered to generate the superchannels, at the expense of flexibility [18], [19]. In particular, in this work the optical transform processor is part of the S-BVT in order to efficiently aggregate the different slices and create a single high capacity flow/superchannel. However, additional processors (i.e. SSSs) can be also included at the network nodes, after the switching matrix, promoting an efficient resource network usage/allocation. The superchannel can be disaggregated at intermediate network nodes and the corresponding demultiplexed slices can be sent to different bandwidth variable receivers (BVRxs), located at different network nodes, for correct demodulation/demapping.

In this paper, an evolutionary SDN-enabled S-BVT architecture based on hybrid electro-optical MCM scheme is proposed and experimentally validated in a photonic mesh network testbed. In comparison with [11], the proposed S-BVT architecture enhances the system programmability/flexibility, modularity and ef-

iciency. Specifically, different optical transceiver implementations can be suitably selected according to the network condition. Thus, the system cost can be reduced by selecting a cost-efficient solution based on DD. Additionally, the optical orthogonal transform processor can be programmed to efficiently multiplex/demultiplex the transmitted/received flows enhancing the system flexibility/efficiency at the expenses of increased complexity. In particular, in section II, the proposed architecture of the SDN-enabled sliceable bitrate variable transceiver, deployed and scaled on demand according to the network condition/requirements, is presented. Section III is devoted to explain the superchannel generation based on the IDWPT/DWPT implementation. In section IV, a proof of the proposed networking concept is performed by transmitting, through different fiber links/paths, a high capacity single flow. In particular, it consists of two DMT signals (S_1 and S_2), aggregated into a superchannel by implementing the DWPT with the Haar wavelet. In this section, the transceiver control aspects are also analyzed and assessed. Finally, in section V, the conclusions are drawn.

II. SDN-ENABLED S-BVT ARCHITECTURE

In Fig. 1, the building blocks of the proposed SDN-enabled S-BVT are described. Specifically, multiple transceiver configurations can be enabled, depending on the network requirements, trading off system performance versus complexity/cost. Accordingly, cost-effective schemes based on IM and DD are envisioned to satisfy the stringent network costs. Whereas, hybrid solutions, consisting of a simple and cost-effective scheme based on AM for the transmitter and a CO receiver, can be considered to enhance resilience against transmission impairments. Specifically, a CO reception enhances robustness against transmission impairments, maximizing the data rate at the increase of the achievable reach.

The proposed programmable sliceable bandwidth variable transmitter (S-BVTx) consists of an adaptive BVTx array (see Fig. 1). At the digital signal

processing (DSP) level, different multicarrier signals are created and converted to analog by means of digital to analog converters (DACs). Specifically, DMT modulation is implemented further enhancing the system flexibility and network dynamicity. Alternative schemes, such as OFDM can also be considered by including at the transmitter/receiver DSP an upconversion/downconversion block in order to generate a real-valued signal. The same spectral efficiency than DMT can be achieved by selecting a radio frequency of half the signal bandwidth [20]. The multicarrier DSP block includes data parallelization and mapping, training symbol insertion, inverse fast Fourier transform (IFFT) implementation, cyclic prefix (CP) insertion and serialization. Additionally, the Levin Campello (LC) BL/PL algorithm is applied in order to flexibly allocate different power values and modulation formats to the different subcarriers according to the channel profile, which is obtained by estimating the signal-to-noise ratio (SNR) of each subcarrier [9], [20]. Hence, the impact of transmission impairments (e.g. CD) and hardware limitations (e.g. DAC bandwidth) on the system performance can be reduced [20]. Different loading algorithms can be applied including LC-rate adaptive (RA) or LC-margin adaptive (MA) [9]. Specifically, the LC-RA algorithm maximizes the system capacity for a fixed/target performance. Whereas, LC-MA maximizes the performance for fixed rate. In both cases, the algorithm has as an input a gap approximation of the SNR (in dB), which is used to relate the number of bits per symbol and the required SNR to achieve a target error probability [9]. The front-end modules can include multiple tunable lasers, to generate a set of orthogonal optical carriers, and external optical modulators such as Mach-Zehnder modulators (MZMs). Alternatively, cost/power efficient schemes, such as multi-wavelength locked lasers and PICs, can be adopted for generating the optical subcarriers [18], [21]. Then, the optical signal/slices can be multiplexed into a single flow with an optical orthogonal transform processor based on either the IFFT or the inverse DWPT (IDWPT) in order to create a spectrally efficient superchannel [14]. Both transforms can be implemented by using programmable SSSs or PICs [22]. After the IDWPT processor, the multiplexed optical flow is transmitted through the network to a destination node. On the other hand, the receiver relies on a modular approach and the SDN agents can suitably enable/disable the corresponding BVRx configuration based on either DD or CO detection according to the network targets/requirements. The signal demultiplexing takes place by implementing the optical FFT/DWPT. Hence, the DMT signal can be distributed to the different BVRxs, as depicted in Fig. 1. After the photodetection stage at each BVRx, the analog signal is digitalized with an analog to digital converter (ADC). Finally, the DSP modules include parallelization, cyclic prefix removal, FFT implementation, equalization, sym-

bol demapping and serialization. In the case of CO-reception, a first module for carrier recovery is also included at the DSP block, as seen in Fig. 1.

On the other hand, an SDN controller will be in charge of managing the network and its elements, including the S-BVT. In fact, multiple transceiver/network elements can be dynamically configured and adapted, according to the requested demand and network path to be supported for an efficient resource usage (see Fig. 1). For instance, the signal bandwidth, laser power/central wavelength and SSS attenuation/phase, between others are parameters that can be configured by means of SDN agents. The agent's purpose is to map high-level operations coming from an SDN controller into low-level, hardware-dependent operations. This involves defining an information and data model for the S-BVT also identifying the parameters that can be reconfigured (see Fig. 6). Hence, a yet another next generation (YANG) common data modeling language has been used in section 6 to detail the configuration data of the proposed S-BVT, describing the network/system elements to be controlled and managed [23]. The YANG modeling provides a standard way to control/manage network elements independently from the vendor, enabling transmission and interoperability in a multi-vendor disaggregated scenario [24].

III. SPECTRALLY EFFICIENT SUPERCHANNEL GENERATION

By the adoption of the flexi-grid paradigm, multiple slices, forming a superchannel, can be efficiently allocated in the network, occupying multiple 12.5 GHz frequency slots [6], [7]. The multiplexing/demultiplexing of the different slices can be performed with optical orthogonal transform processors such as SSSs or even with PICs, in order to emulate the IDWPT/DWPT (see Fig. 1). The adoption of SSSs allows a higher degree of flexibility as the suitable wavelet can be programmed/configured according to the network condition. However, in [19], an integrated processor (based on PICs), that can also be programmed to perform a variety of functions by implementing a common hardware platform, has been proposed. Therefore, it probably could also be reconfigured by the control plane bringing a high level of flexibility. On the other hand, the DWPT of a discrete sequence can be numerically evaluated via recursive discrete convolutions with a low and a high pass filter followed by subsampling factor of 2, giving the details and the scaling coefficients, which are the orthogonal projections of the input sequence. In particular, the IDWPT/DWPT consists of a chain/tree of half-band and quadrature mirror filters, which can be synthesized by directly using cascaded Mach-Zehnder interferometers (MZIs), with initial differential path delay of τ , equal to the inverse of the free spectral range (FSR) [22]. The MZIs can be integrated

employing different technologies, such as silicon-on-insulator, further enhancing power efficiency [22]. For instance, Fig. 2 shows a PIC-based IDWPT/DWPT optical orthogonal processor that we have designed and it has been processed on a standard silicon wafer. The proposed PIC design has been produced on a generic photonic integration platform based on silicon nitride. In particular, we have implemented an optical architecture of a IDWPT/DWPT decomposition up to the second level, where each filter/MZI supports the Haar wavelet. In the case of implementing the IDWPT, the first decomposition level consists of 2 MZIs with initial path delay of 2τ . Whereas, in the last decomposition level there is a single MZI with initial path delay of τ , according to [25]. By adopting this optical orthogonal PIC-based processor up to 4 signals/slices can be efficiently packed into a superchannel, enabling high data rate transmission over the network with a radical reduction of cost, power consumption and footprint.

Alternatively, in order to implement either the DWPT or the IDWPT to create an optical spectrally-efficient superchannel, the SSS should be suitably programmed by setting the appropriate frequency response (attenuation/phase) of each port to fix different MZI-based filter transfer functions, depending on the selected wavelet bases. Multiple wavelet transfer functions can be programmed according to the network targets. For instance, the transfer function of the Haar wavelet, synthesized considering a FSR of 40 GHz (related to the delay between the MZI arms), can be seen in Fig. 3 (a). In particular, one filter output (solid line) has a maximum at the central carrier frequency of one slice ($\lambda_1 = 1549.96$ nm) and a null at the central carrier frequency of the neighbor slice ($\lambda_2 = 1550.12$ nm). Whereas, the other filter output (dashed line) presents the opposite behavior. The multiplexed signals, after applying the selected MZI transfer function of Fig. 3 (a), can be seen in Fig. 3 (b). From the figure, it can be observed that the two orthogonal signals have been suitably packed by implementing the IDWPT with Haar wavelet forming a superchannel with a total bandwidth occupancy of 40 GHz. In the particular case of having a superchannel with only two optical/orthogonal carriers, the single Haar-based wavelet packet stage can also be implemented with a simple 3 dB coupler, simplifying the S-BVT architecture [14].

IV. PROOF OF CONCEPT

In order to experimentally assess the feasibility of the proposed solution, two S-BVT building blocks, based on DMT transmission are enabled. Two possible receiver architectures based on either DD or CO have been experimentally evaluated. Two tunable laser sources centered at 1550.12 nm and 1549.96 nm are used to create orthogonal tones. Electrical DMT



Fig. 2. PIC-based IDWPT/DWPT optical orthogonal transform processors corresponding to a 2-levels decomposition Haar wavelet

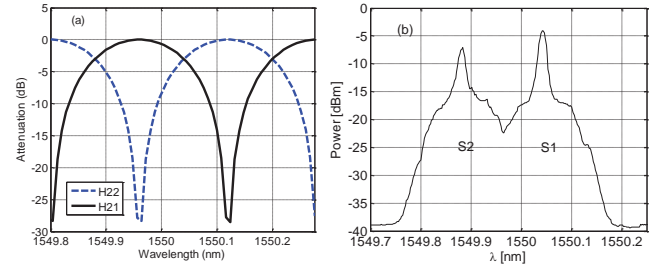


Fig. 3. (a) MZI transfer function emulating the Haar wavelet and considering 40 GHz FSR (b) OSA capture of the two multiplexed slices with a 0.4 nm resolution bandwidth

signals with 10 GHz bandwidth occupancy are digitally generated and converted to analog with an arbitrary waveform generator (AWG) working at 20 GS/s with 10 GHz bandwidth. The experimentally measured transfer function of the AWG is presented in the inset (a) of Fig. 4. At the DSP level, a randomly generated data stream is parallelized and mapped into different modulation formats, including BPSK and optimized m -QAM constellations ($m = 2^l$; $2 \leq l \leq 8$), according to the BL/PL algorithm for adaptive mapping [20]. The SNR per subcarrier is estimated to activate the BL/PL algorithm (LC-RA) in order to adapt/reconfigure the transmitter to maximize system capacity [20]. An example of the resulting SNR estimation and bit assignment per subcarrier for the implementation of AM/CO, after 25 km of standard single mode fiber (SSMF), can be seen in the insets (b) and (c) of Fig. 4, respectively. In particular, the high frequency subcarriers present slightly SNR degradation due to the limited bandwidth of the AWG (see also inset (a) of Fig. 4). Then, 4 training symbols are added to correctly equalize the data at the receiver side. A 512-point inverse FFT is performed to create orthogonal subcarriers, where only 256 subcarriers carry data to implement the hermitian symmetry required in DMT modulation. Before serialization and upconversion processes, a cyclic prefix of 1.9% overhead is added at the beginning of each DMT symbol. Two external MZMs, which optically modulate the two DMT signals, work near the null point and at the quadrature point for AM and IM,

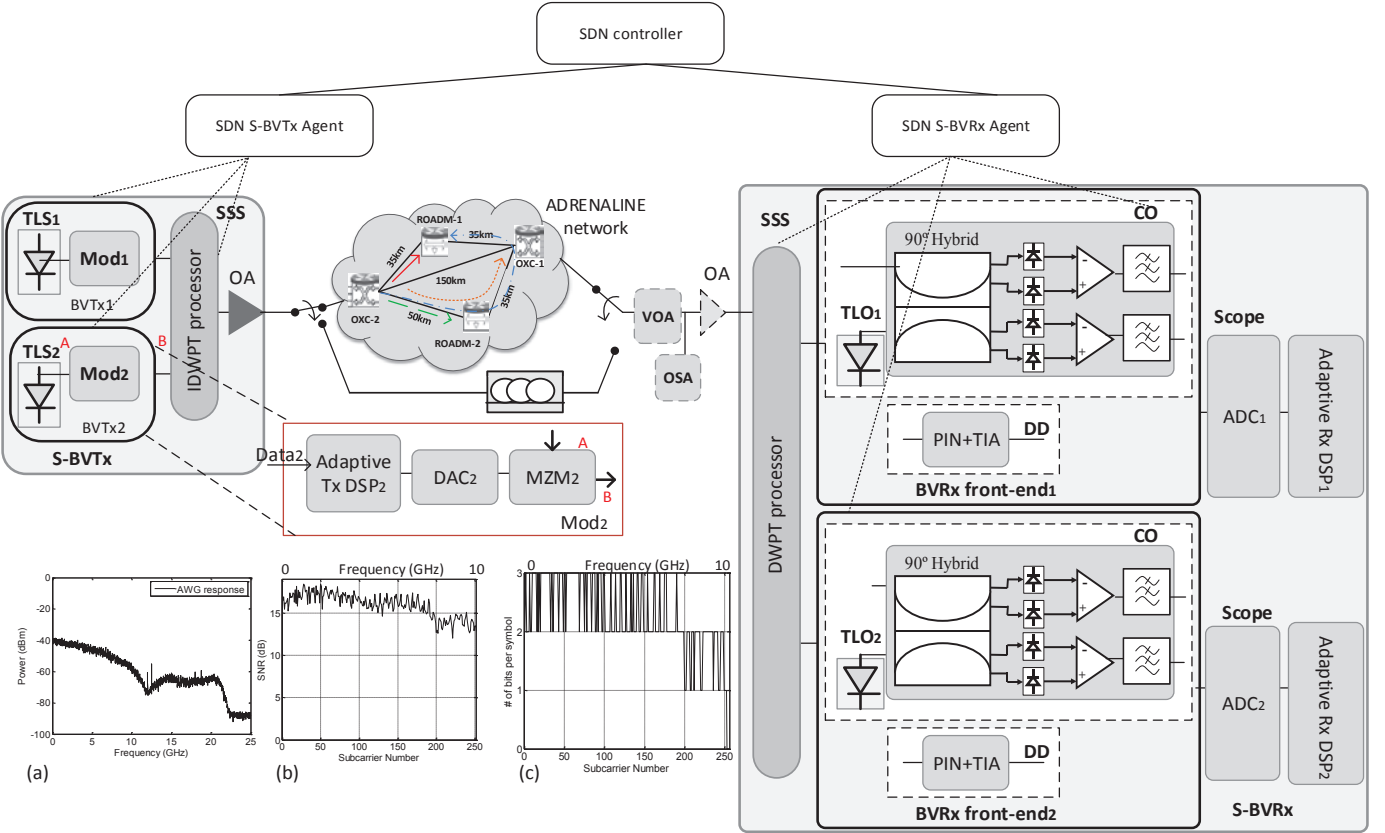


Fig. 4. Experimental set-up for the proof of concept. In the inset of the figure, (a) AWG transfer function and example of (b) estimated SNR and (c) bit assignment per subcarrier considering AM and CO reception

respectively. Then, an SSS is included to efficiently aggregate the two optical DMT signals by programming the attenuation and phase per port. The SSS acts as an optical transform processor by emulating the IDWPT considering the transfer function of the Haar wavelet of Fig. 3 (a). The generated superchannel is transmitted over different fiber spools and the ADRENALINE photonic mesh network, which consists of 4 optical nodes interconnected with different SSMF links [26]. At the destination node, the suitable receiver (DD or CO configuration) is selected according to the network condition. Then the SSS is used to demultiplex the received superchannel and distribute the resulting DMT signals to the bank of BVRxs. In the case of DD reception, each disaggregated signal is photodetected with a PIN, followed by a transimpedance amplifier (TIA), and analog to digital converted with a real-time oscilloscope running at 100 GS/s. Finally, the original bit stream is recovered after being digitally processed by the corresponding DMT DSP block. When a phase diversity CO front-end is used, which enables the detection of the full optical field, the demultiplexed signals are mixed with each tunable local oscillator (TLO) in a 90° degree hybrid. The same optical source is used at the transmitter and as local oscillator at the receiver side. A couple of balanced photodetectors are then used to convert the optical signal to electri-

cal. Finally, a real-time oscilloscope, also running at 100 GS/s, is used for analog-to-digital conversion and the corresponding DSP to recover the original data.

According to Fig. 4, the slice aggregation/disaggregation is performed by the DWPT processor. Therefore, another DWPT/SSS can be included at the network nodes, promoting a dynamic use of the spectrum. Hence, different slices can be transmitted through different network paths and multiplexed/demultiplexed at an intermediate network nodes. The control plane can set up the suitable SSS configuration by means of SDN agents.

A. Experimental assessment

The proposed set-up of Fig. 4 has been experimentally validated over different optical paths up to 120 km of SSMF. Hence, the system performance is evaluated in terms of achieved data rate when transmitting a superchannel, consisting of two multiplexed slices, occupying 4 slots of 12.5 GHz granularity in a flex-grid scenario. The ADRENALINE testbed is used to assess the transmission of the aggregated flow over a metro network scenario. Multiple network paths have been tested including 1-hop path of 35 km and 50 km, 2-hops path of 85 km and a 3-hops path of 120 km, depicted in Fig. 4 and summarized in table I. On the other hand, the superchannel

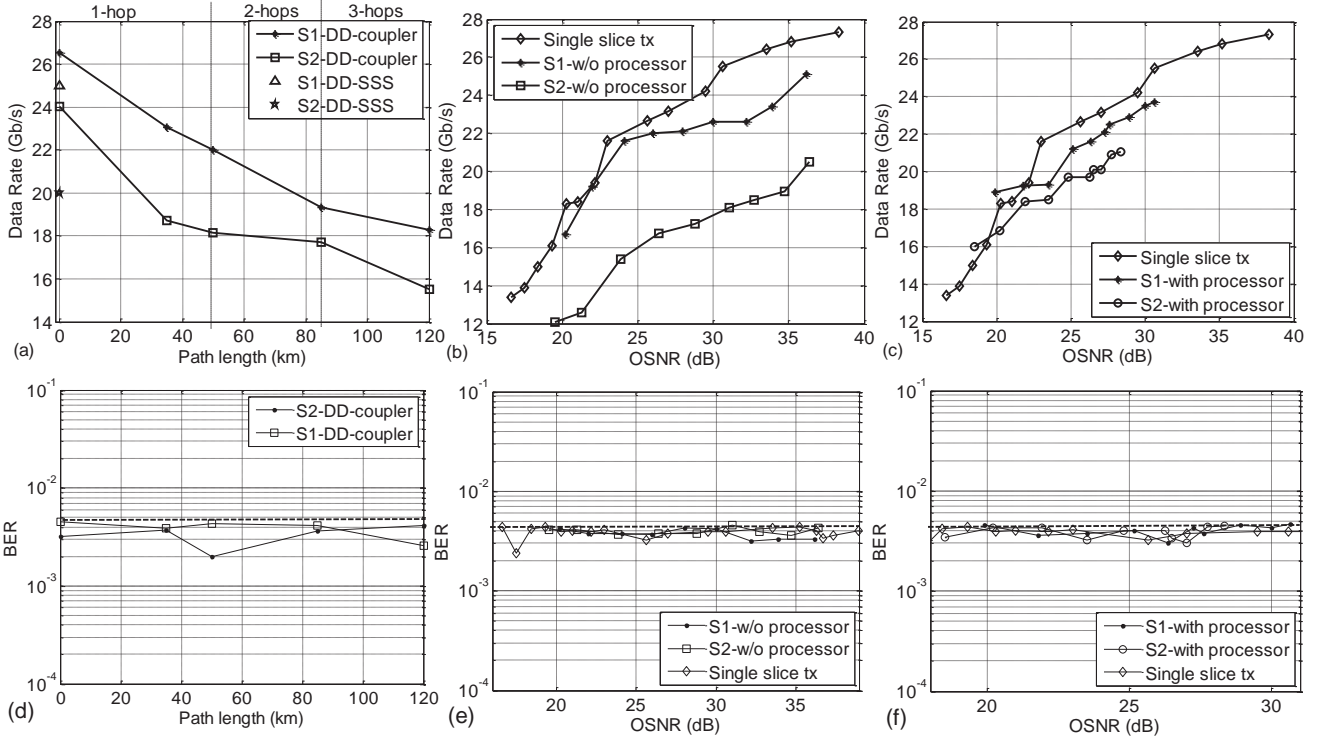


Fig. 5. (a) Achieved data rate versus optical path for IM/DD and with 3 dB coupler for superchannel generation. In B2B configuration, a maximum OSNR of 34 dB (S1-DD-coupler), 31 dB (S1-DD-SSS), 33 dB (S2-DD-coupler) and 26 dB (S2-DD-SSS) is obtained. (b,c) Achieved data rate versus OSNR, with CO reception after 25 km of SSMF without and with optical orthogonal transform processor configured with the Haar transform. (d) Achieved BER vs path for IM/DD and with 3 dB coupler for superchannel generation. (e, f) Achieved BER versus OSNR, with CO reception after 25 km of SSMF without and with optical orthogonal transform processor configured with the Haar transform

is generated by suitably programming the SSSs to emulate the IDWT/DWPT with the Haar transform, which is the simplest wavelet. As a first step, IM/DD implementation is configured, also considering a simple 3 dB coupler for superchannel generation. In our previous work, [14], it has been demonstrated that equal/similar performance is achieved by multiplexing two signals/slices with a 3 dB coupler or with an SSS emulating the Haar wavelet. From Fig. 5 (a), it can be seen that an aggregated data rate of 50 Gb/s can be achieved in back-to-back (B2B) with 34 dB OSNR, when considering a simple coupler as optical orthogonal transform processor. By suitably programming the SSS for multiplexing the two slices with the Haar wavelet, 25 Gb/s and 20 Gb/s are independently achieved, requiring a maximum OSNR of 31 dB and 26 dB, respectively. For the same OSNR values, similar results are achieved considering the coupler as shown in [14]. The performance difference in terms of data rate between the two slices is mainly due to the set-up implementation. Specifically, two different MZMs have been used to optically modulate the electrical DMT signals, as it can be seen from the spectra of the two transmitted slices in Fig. 3 (b). As shown in Fig. 5 (a) the data rate of both slices decreases after passing through different network nodes. The data rate penalty, with respect to B2B configuration, when transmitting through different network paths

considering IM/DD configuration is summarized in table I. In the case of considering a single-hop scenario, a minimum data rate penalty, with respect to the B2B configuration, of about 13% is observed, for S1, after the 35 km path (OXC-2 \rightarrow ROADM-1). Whereas a maximum penalty of 24.5% can be seen, for S2, after the 50 km path (OXC-2 \rightarrow ROADM-2). After a 3-hops path (OXC-2 \rightarrow ROADM-2 \rightarrow OXC-1 \rightarrow ROADM-1), of a total length of 120 km over the ADRENALINE testbed, the data rate of both slices decreases 8.22 Gb/s and 8.5 Gb/s, respectively (corresponding to 31% and 35.4% penalties). In this case, the chromatic dispersion of the fiber limits the system performance, and hence data rate degradation is observed. However, thanks to the implementation of BL/PL algorithms, which suitably assign different bits and power values per subcarrier according to the channel profile, the target BER can be ensured for all the analyzed cases as seen in Fig. 5 (d).

On the other hand, Fig. 5 (b) and (c) show the achieved data rate versus OSNR by setting up AM with CO reception after transmitting over 25 km of SSMF. Negligible data rate penalty is achieved with respect to B2B. In fact, according to [27], the considered scheme based on AM/CO shows high robustness against accumulated dispersion up to 150 km of SSMF. By implementing a bandpass filter (BPF) at the SSS, namely without the optical transform processor, a data rate penalty of 2 Gb/s and 7 Gb/s is evidenced at

TABLE I

DATA RATE PENALTY, WITH RESPECT TO THE B2B CONFIGURATION, OVER DIFFERENT NETWORK PATHS FOR IM/DD CONFIGURATION

Path	Length [km]	S1 Penalty [%]	S2 Penalty [%]
OXC-2 →ROADM-1	35	13	22
OXC-2 →ROADM-2	50	16.9	24.5
OXC-2 →ROADM-2 →OXC-1	85	27.1	26.1
OXC-2 →ROADM-2 →OXC-1 →ROADM-1	120	31	35.4

each slice at 29 dB OSNR, when compared to the case of transmitting a single slice, as seen in Fig. 5 (b). Depending on the SSS configuration, one slice could be more affected than the other. For instance, by choosing a specific filter bandwidth and central wavelength per port and taking into account that there is no guard band between the slices, one slice can be more degraded due to the edge of the filter. Whereas by programming the optical transform processor/SSS considering the transfer function of Fig. 3 (a), in order to emulate the Haar wavelet, this penalty is reduced to 1 Gb/s and 3 Gb/s for each slice at the same OSNR value, as observed in Fig. 5 (c). It is important to take into account that similar performance in terms of data rate is achieved for both slices when considering the optical processor. However, less than 2 Gb/s penalty is observed between both contributions due to setup implementation. Specifically, the two slices are generated with two different MZMs. From Fig. 5 (e) and (f), it can be observed that the target BER is ensured for all the analyzed cases. Multiple DMT signals can be also aggregated/multiplexed further increasing system's capacity and scalability/flexibility at the expense of OSNR. Inter-channel interference is mitigated by the adoption of orthogonal optical transform processors.

B. Transceiver control aspects

The programmable parameters of the SDN-enabled S-BVT have been identified enabling the control plane to configure the transceiver according to the network requirements. The reconfiguration time of the S-BVT can be up to 90 seconds, as offline DSP is employed. The YANG model of the proposed S-BVT can be visualized through a compact tree and the corresponding UML diagram in Fig. 6. On the one hand, the *slice-id*, *bandwidth* occupation/selection, the *central-wavelength*, forward error correction (*FEC*), *bit-rate* per slice, *DSP-mode* and BL/PL algorithm (*name*, *gap* and *SNR*) parameters can be suitably programmed for slice configuration/operation, promoting an intelligent management of the optical network.

In particular, the DSP-mode field can be suitably set to signal-to-noise ratio (SNR) estimation or data transmission operation modes. The SNR estimation is selected in order to automatically map all the DMT subcarriers with the same modulation format. Next, at the receiver, the noise and power of each received symbol are calculated and further averaged per subcarrier

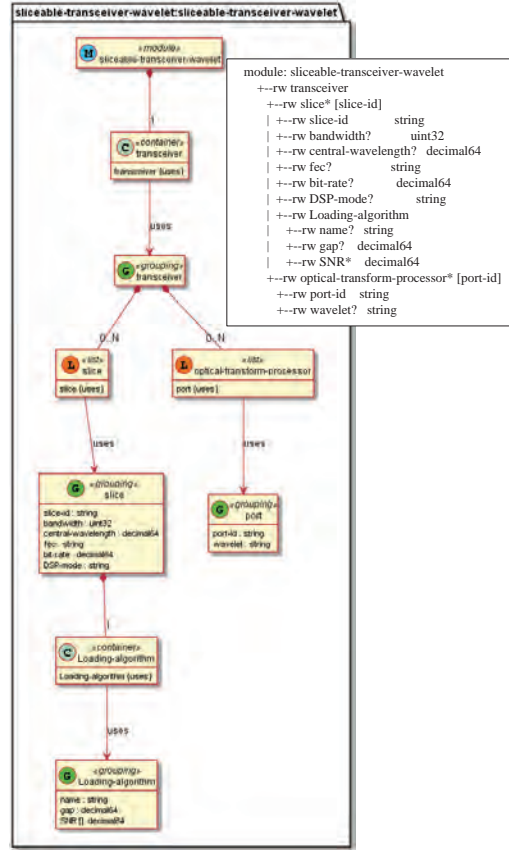


Fig. 6. S-BVT YANG model in UML

in order to estimate the channel profile. The obtained channel information (*SNR* parameter) is collected by the corresponding SDN agent and passed to the SDN controller, and send back to the transmitter, whose SDN agent uses this data to adjust/set the number of bits and power values per subcarrier, according also to the selected BL/PL (*name*) algorithm (i.e. margin adaptive, MA, or rate adaptive, RA), and *SNR gap* (required to initialize the algorithm and fix a target performance) [9]. Then, the S-BVT is set to operate in transmission mode, ensuring that the optimum modulation format and power values are used.

On the other hand, other system/network elements such as the optical transform processor (i.e. the SSS, which is part of the S-BVT) can be appropriately configured, by the SDN controller by means of SDN agents to implement the suitable wavelet base (as seen in Fig. 6). In the case of using the SSS, by choosing specific *port-id* and *wavelet* and taking into

Time	Source	Destination	Protocol	Length	Info
8 0.137085155	NET_SDN_CTRL	SDN_AGENT	HTTP	4181	POST /agent/restconf/data
10 0.043044271	SDN_AGENT	NET_SDN_CTRL	HTTP	196	HTTP/1.1 201 Created

```

+ Member Key: sliceable-transceiver-wavelet:transceiver
- Object
+ Member Key: slice
- Array
+ Object
+ Member Key: slice-id
  String value: 1
  Key: slice-id
+ Member Key: bandwidth
+ Member Key: central-wavelength
+ Member Key: fec
+ Member Key: bit-rate
+ Member Key: DSP-mode
+ Member Key: Loading-algorithm
+ Object
+ Member Key: slice-id
  String value: 2
  Key: slice-id
+ Member Key: bandwidth
+ Member Key: central-wavelength
+ Member Key: fec
+ Member Key: bit-rate
+ Member Key: DSP-mode
+ Member Key: Loading-algorithm
Key: slice
+ Member Key: optical-transform-processor
- Array
+ Object
+ Member Key: port-id
  String value: 1
  Key: port-id
+ Member Key: wavelet
  String value: Haar
  Key: wavelet
+ Object
+ Member Key: port-id
  String value: 2
  Key: port-id
+ Member Key: wavelet
  String value: Haar
  Key: wavelet
Key: optical-transform-processor

```

Fig. 7. Sample JSON object corresponding to the configuration of the S-BVT.

Time	Source	Destination	Protocol	Length	Info
6 0.100894158	SDN_AGENT	NET_SDN_CTRL	HTTP	93	HTTP/1.1 100 Continue
8 0.101052708	NET_SDN_CTRL	SDN_AGENT	HTTP	4181	POST /agent/restconf/data
10 0.940257222	SDN_AGENT	NET_SDN_CTRL	HTTP	196	HTTP/1.1 201 Created

```

+ Member Key: sliceable-transceiver-wavelet:transceiver
- Object
+ Member Key: slice
- Array
+ Object
+ Member Key: slice-id
  String value: 1
  Key: slice-id
+ Member Key: bandwidth
  Number value: 10
  Key: bandwidth
+ Member Key: central-wavelength
  Number value: 1550.12
  Key: central-wavelength
+ Member Key: fec
  String value: HD-FEC_4.62e-3
  Key: fec
+ Member Key: bit-rate
  Number value: 0
  Key: bit-rate
+ Member Key: DSP-mode
  String value: Data transmission
  Key: DSP-mode
+ Member Key: Loading-algorithm
+ Object
+ Member Key: name
  String value: LC-RA
  Key: name
+ Member Key: gap
  Number value: 9
  Key: gap
+ Member Key: SNR
- Array
  Number value: 16.41
  Number value: 16.90
  Number value: 15.42
  Number value: 16.10
  Number value: 16.13
  Number value: 16.38
  Number value: 16.69
  Number value: 15.24

```

Fig. 8. Sample JSON object corresponding to the configuration of a single slice.

account the *central-wavelength* and *bandwidth* slice parameters, the SDN agent can identify in a look-up table the required attenuation and phase configuration to be applied at each port in order to implement the target wavelet transfer function. Alternatively, other programmable optical transform processors can be considered such as photonic integrated signal processors [19], which can also be reconfigured by software in order to program the suitable wavelet. In the case

of having an additional optical transform processor as part of the network node, this can also be configured with the suitable transform in order to correctly multiplex/demultiplex the superchannel and deliver the resulting slices/flows to the different destination nodes.

Finally, a sample configuration of the programmable SDN-enabled S-BVT using RESTCONF and JSON data format is shown in Fig. 7. RESTCONF is used as an SDN protocol for the control of optical networks, by exploiting the YANG data model, to describe the network elements to be controlled/managed. From the figure it can be seen the configuration of the S-BVT, including two slices and two ports of the SSS. The two slices can be configured by programming the identified parameters. For the configuration of the SSS, the *wavelet* parameter of both ports (*port-id*=1 and *port-id*=2) is set to Haar. Thus, the corresponding transfer function (phase/attenuation) per port will be configured according to a look-up table.

From Fig. 8, it can be seen in more detail the configuration of one of the slices (*slice-id*=1). Specifically, the *central wavelength* parameter is set to 1550.12 nm, the slice *bandwidth* is fixed at 10 GHz and the *FEC* is set to hard decision (HD)-FEC (corresponding to a 7% overhead) targeting $4.62 \cdot 10^{-3}$ BER. Additionally, the *DSP-mode* parameter is set to data transmission mode, enabling the implementation of the selected loading algorithm. The *name* parameter of the loading algorithm is set to LC-RA with an initial *gap* value of 9 dB. The last required parameter, to configure one slice of the S-BVT, is the *SNR*. In Fig. 8, it can be seen an example of the estimated SNR values corresponding to the first low frequency subcarriers. Lower SNR values are estimated for high frequency subcarriers due to hardware limitations (i.e. AWG limited bandwidth). Similar parameters are configured to the other slice (*slice-id*=2), with the difference that the *central wavelength* parameter is set to 1549.96 nm.

V. CONCLUSIONS

In this work, a programmable SDN-enabled S-BVT based on optical orthogonal transform processor has been proposed as key enabler for superchannel generation enabling flexible/efficient transmission within optical metro networks. Super/sub-wavelength granularity has been exploited by considering a hybrid electro-optical MCM scheme. The proposed transceiver based on multiple optical implementations, including IM/DD and AM/CO, has been experimentally validated trading-off system performance and cost-effectiveness. Specifically, by the adoption of CO high robustness against accumulated dispersion is achieved. System/network programmability is fully exploited by suitably implementing SDN agents that configure the proposed S-BVT. Successful transmission over different fiber links have been experimentally assessed for a maximum aggregated data rate of

50 Gb/s at 34 dB OSNR. High data rate transmission over optical metro networks can be envisioned by enabling multiple S-BVT building blocks. Additionally, system/network flexibility can be fully exploited by including programmable SSS at the network nodes. This enables efficient superchannel generation according to the network condition.

VI. ACKNOWLEDGMENTS

We would like to thank VLC Photonics and Centro Nacional de Microelectrónica (CNM) for the fabrication of the proposed PIC-based IDWPT/DWPT optical orthogonal transform processors within a multi-project wafer shuttle run.

REFERENCES

- [1] Cisco Visual Networking Index Global Mobile Traffic Forecast Update, 2016-2021 White Paper.
- [2] SK Telecom, "SK Telecom's View on 5G Vision, Architecture, Technology, and Spectrum", 5G White Paper, (2014).
- [3] NGMN Alliance, "NGMN 5G White Paper", Feb 2015.
- [4] M. Fiorani, P. Monti and B. Skubic, "Challenges for 5G transport networks", in ANTS, 2014.
- [5] Telefónica and Ericsson, "Cloud RAN Architecture for 5G", White paper.
- [6] ITU-T Recommendation G.694.1, 2012.
- [7] A. Napoli, M. Bohn, D. Rafique, A. Stavdas, N. Sambo, L. Potí, M. Nolle, J. K. Fischer, E. Riccardi, A. Pagano, A. Di Giglio, M. Svaluto Moreolo, J. M. Fabrega, E. Hugues-Salas, G. Zervas, D. Simeonidou, P. Layec, A. D'Errico, T. Rahman, and J. P. Fernández-Palacios, "Next generation elastic optical networks: The vision of the European research project IDEALIST", in IEEE Communications Magazine, vol. 53, no. 2, pp. 152-162, Feb. 2015.
- [8] A. Sano and Y. Miyamoto, "Ultra-high speed optical OFDM transmission technologies", Conf. on Optical Internet, Tokyo, 2008.
- [9] L. Nadal, M. Svaluto Moreolo, J. M. Fàbrega, A. Dochhan, H. Griebner, M. Eiselt, J.-P. Elbers, "DMT Modulation with Adaptive Loading for High Bit Rate Transmission Over Directly Detected Optical Channels", in JLT, Vol. 32, No. 21, pp. 3541-3551, November 2014.
- [10] Ben Ezra, A. Zadok, R. Califa, D. Munk and B. I. Lembrikov, "All-optical wavelet-based orthogonal frequency division multiplexing system based on silicon photonic integrated components", IET Optoelectronics, 2016, 10, (2), p. 44-50
- [11] N. Sambo, P. Castoldi, A. D'Errico, E. Riccardi, A. Pagano, M. Svaluto Moreolo, J. M. Fàbrega, D. Rafique, A. Napoli, S. Frigerio, E. Hugues Salas, G. Zervas, M. Nolle, J. K. Fischer, A. Lord, J. P. F. -P Giménez, "Next generation sliceable bandwidth variable transponders", IEEE Comm. Magaz., Vol.53, no. 2, p. 163-171, 2015.
- [12] R. Casellas, J. M. Fabrega, R. Munoz, L. Nadal, R. Vilalta, M. Svaluto Moreolo and R. Martinez, "On-Demand Allocation of Control Plane Functions via SDN/NFV for Monitoring-enabled Flexi-grid Optical Networks with Programmable BVTs," in proceedings of ECOC, Dusseldorf, Germany, 2016.
- [13] J. M. Fàbrega, M. Svaluto Moreolo, A. Mayoral, R. Vilalta, R. Casellas, R. Martínez, R. Muñoz, Y. Yoshida, K. Kitayama, Y. Kai, M. Nishihara, R. Okabe, T. Tanaka, T. Takahara, J. C. Rasmussen, N. Yoshikane, X. Cao, T. Tsuritani, I. Morita, K. Habel, R. Freund, V. López, A. Aguado, S. Yan, D. Simeonidou, T. Szyrkowiec, A. Autenrieth, M. Shiraiwa, Y. Awaji and N. Wada, "Demonstration of Adaptive SDN Orchestration: A Real-Time Congestion-Aware Services Provisioning Over OFDM-Based 400G OPS and Flexi-WDM OCS", J. Lightwave Technol. 35, 506-512 (2017).
- [14] L. Nadal, M. Svaluto Moreolo, J. M. Fàbrega and F. J. Vilchez, "Hybrid Electro-Optical MCM as Multi-Flow Generation Enabler for Elastic Optical Networks", CLEO EUROPE, CI-5.1, 2017.
- [15] A. Li, W. Shieh and R. S. Tucker, "Wavelet Packet Transform-Based OFDM for Optical Communications", in JLT, vol. 28, no. 24, pp. 3519-3528, Dec.15, 2010.
- [16] D. Hillerkuss, M. Winter, M. Teschke, A. Marculescu, J. Li, G. Sigurdsson, K. Worms, S. Ben Ezra, N. Narkiss, W. Freude and J. Leuthold, "Simple all-optical FFT scheme enabling Tbit/s real-time signal processing", Opt. Express 18, 9324-9340 (2010)
- [17] A. Li, W. Shieh and Rodney S. Tucker, "Wavelet Packet Transform-Based OFDM for Optical Communications", in JLT, vol. 28, no. 24, pp. 3519-3528, Dec.15, 2010.
- [18] A. D'Errico and G. Contestabile, "Next Generation Terabit Transponder", in OFC, paper W4B.4, 2016.
- [19] J. Capmany, I. Gasulla and D. Pérez, "Microwave photonics: The programmable processor", in Nature Photonics, 10, pp. 6-8, 2016.
- [20] L. Nadal, M. Svaluto Moreolo, J. M. Fàbrega and F. J. Vilchez, "Meeting the future metro network challenges and requirements by adopting programmable S-BVT with direct-detection and PDM functionality", OFT, Vol. 36, July (2017).
- [21] M. Imran, P. M. Anandarajah, A. Kaszubowska-Anandarajah, N. Sambo and L. Potí, "A Survey of Optical Carrier Generation Techniques for Terabit Capacity Elastic Optical Networks", in IEEE Communications Surveys and Tutorials, vol. 20, no. 1, pp. 211-263, 2018.
- [22] M. S. Moreolo, G. Cincotti and A. Neri, "Synthesis of optical wavelet filters", in IEEE PTL, vol. 16, no. 7, pp. 1679-1681, July 2004.
- [23] M. Dallaglio, N. Sambo, F. Cugini, and P. Castoldi, "Control and Management of Transponders With NETCONF and YANG," J. Opt. Commun. Netw. 9, B43-B52 (2017).
- [24] M. De Leenheer, T. Tofigh, and G. Parulkar, "Open and Programmable Metro Networks", in Proc. OFC 2016, paper Th1A.7.
- [25] M. S. Moreolo and G. Cincotti, "Compact low-loss planar architectures for all-optical wavelet signal processing", ICTON, paper Tu.B2.7, 2005.
- [26] R. Munoz, L. Nadal, R. Casellas, M. Svaluto Moreolo, R. Vilalta, J. M. Fàbrega, R. Martínez, A. Mayoral and Fco. J. Vilchez, "The ADRENALINE Testbed: An SDN/NFV Packet/Optical Transport Network and Edge/Core Cloud Platform for End-to-End 5G and IoT Services", in EUCNC, June, 2017.
- [27] J. M. Fàbrega, M. Svaluto Moreolo, F. J. Vilchez, K. Christodoulopoulos, E. Varvarigo, and J. P. Fernández-Palacios, "Experimental validation of MTU-BRAS connectivity with DMT transmission and coherent detection in flexgrid metro networks using sliceable transceivers", in OFC, paper Th3H.4, 2015.

Laija Nadal obtained her MSc Telecommunication Engineering degree from UPC-BarcelonaTech university in July 2010. She obtained the European Master of Research on Information and Communication Technologies (MERIT) from the Signal Theory and Communications (TSC) department of the UPC in 2012. She received her PhD degree from TSC department of the UPC in November 2014. In 2010, she was awarded with the FPI grant from the Spanish Ministry of Economy and Competitiveness (MINECO) to perform her PhD within the framework of the National project DORADO in the CTTC. From May to August 2013 she was a Visiting Ph.D. Scholar in ADVA Optical Networking (Germany). She currently is a Researcher of the Communication Networks Division. Her research interests include signal processing and advance modulation formats for optical communication systems.

Michela Svaluto Moreolo (IEEE S'04-A'08-SM'13) received the M.Sc. degree (with honors) in electronics engineering and Ph.D. degree in telecommunications engineering from University Roma Tre, Rome, Italy, in 2003 and 2007, respectively. In 2004, she became a Teaching Assistant at Engineering Faculty, University Roma Tre, and from January to July 2004, she was a Visiting Researcher at the Institute of Semiconductor and Solid State Physics, Johannes Kepler University, Linz, Austria. From January 2007 to December 2008, she held a Postdoctoral position at the Applied Electronics Department, University Roma Tre. In January 2009, she joined CTTC. She is currently a Senior Researcher of the Communication Networks Division and the Coordinator of the Optical Transmission and Subsystems research line within the Optical Networks and Systems Department. Since September 2016, she is also a member of the Management Team of the CTTC, with the role of Project Management Coordinator. Her research interests include advanced modulation formats and software-defined transmission technologies for future optical networks.

Josep M. Fàbrega received his BSc and MSc degrees in telecommunications engineering, and PhD degree in signal theory and communications from UPC-BarcelonaTech, Barcelona, Spain, in 2002, 2006 and 2010 (hons.), respectively. Currently he is a Senior Researcher in the Optical Networks and Systems Department of CTTC, Castelldefels, Spain. Prior to that, he was with the scientific staff of the UPC-BarcelonaTech Optical Communications Group from 2004 to 2010. Since 2004, he has been actively involved in 22 National, EU-funded (FP6, FP7 and H2020) and technology transfer R&D projects. He is the author of more than 30 papers and co-author of another over 70 papers, including 2 patents. His research interests include broadband optical communications emphasizing on advanced modulation formats and optical signal delivery over novel network architectures. Dr. Fabrega is an IEEE Senior Member and received the EuroFOS best student research award for his PhD thesis in 2010.

Ramon Casellas (IEEE SM'12) graduated in telecommunications engineering in 1999 by both the UPC-BarcelonaTech university and ENST Telecom Paristech, within an Erasmus/Socrates double degree program. After working as an undergraduate researcher at both France Telecom R&D and British Telecom Labs, he completed a Ph.D. degree in 2002. He worked as an associate professor at the networks and computer science department of the ENST (Paris) and joined the CTTC Optical Networking Area in 2006, with a Torres Quevedo research grant. He currently is a senior research associate and the coordinator of the ADRENALINE testbed. He has been involved in several international R&D and technology transfer projects. His research interests include network control and management, the GMPLS/PCE architecture and protocols, software defined networking and traffic engineering mechanisms. He contributes to IETF standardization within the CCAMP and PCE working groups. He is a member of the IEEE Communications Society and a member of the Internet Society.

F. Javier Vílchez graduated in Telecommunication Engineering by the Polytechnic University of Catalonia in April 2002, and also graduated in Electronics Engineering by the same school in March 2007. He joined the former CTTC Optical Networking Area (now Optical Networks and Systems Department) in February 2008, as Research Engineer (becoming Researcher in 2013). His work focuses mainly on hardware and firmware design and development for electronic and optical circuits. Furthermore, he is mainly involved on the continuous evolution of ADRENALINE testbed, by the implementation and integration of prototypes based on opto-electronic systems with the required interfaces for the management from the control plane. Since November 2010, he is Coordinator of the Optical Networks and Systems laboratory.

Ricardo Martínez (IEEE SM'14) graduated and PhD in telecommunications engineering by the UPC-BarcelonaTech university in 2002 and 2007, respectively. He has been actively involved in several public-funded (national and EU) R&D as well as industrial technology transfer projects. Since 2013, he is Senior Researcher of the Communication Networks Division (CND) at CTTC. His research interests include control and network management architectures, protocols and traffic engineering mechanisms for next-generation packet and optical transport networks within aggregation/metro and core segments.

Ricard Vilalta graduated in telecommunications engineering in 2007 and received a Ph.D. degree in telecommunications in 2013, both from the Universitat Politècnica de Catalunya (UPC), Spain. He also has studied Audiovisual Communication at UOC (Open University of Catalonia) and is a master degree on Technology-based business innovation and administration at Barcelona University (UB). Since 2010, Ricard Vilalta is a researcher at CTTC, in the Optical Networks and Systems Department. His research is focussed on Optical Network Virtualization and Optical Openflow. He is currently a Research Associate at Open Networking Foundation.

Raül Muñoz (IEEE SM'12) graduated in telecommunications engineering in 2001 and received a Ph.D. degree in telecommunications in 2005, both from the Universitat Politècnica de Catalunya (UPC), Spain. After working as undergraduate researcher at Telecom Italia Lab (Turin, Italy) in 2000, and as assistant professor at the UPC in 2001, he joined the Centre Tecnològic de Telecomunicacions de Catalunya (CTTC) in 2002. Currently, he is Senior Researcher, Head of the Optical Network and System Department, and Manager of the Communication Networks Division. Since 2000, he has participated in several R&D projects funded by the European Commission's Framework Programmes (FP7 FP6 and FP5) and the Spanish Ministries, as well as technology transfer projects. He has led several Spanish research projects, and currently leads the European Consortium of the EU-Japan project STRAUSS. His research interests include control and management architectures, protocols and traffic engineering algorithms for future optical transport networks.